Removal of Hg^0 from Flue Gas Using Two Homogeneous Photo-Fenton-Like Reactions

Yangxian Liu
School of Energy and Power Engineering, Jiangsu University, Zhenjiang, Jiangsu 212013, China

Jun Zhang
Key Laboratory of Energy Thermal Conversion and Control of Ministry of Education, Southeast University, Nanjing 210096, China

Yanshan Yin
Dept. of Hunan Province, Key Laboratory of Efficient and Clean Energy Utilization of Education, Changsha University of Science and Technology, Changsha 410000, China

DOI 10.1002/aic.14727

Removal of Hg^0 using two homogeneous Photo-Fenton-Like reactions was first investigated in a photochemical reactor. Effects of process parameters on Hg^0 removal were studied. Free radical and reaction products were analyzed. Removal pathways of Hg^0 were discussed. Simultaneous removal of Hg^0, NO, and SO_2 is also studied briefly. The results show that UV power, wavelength, H_2O_2 concentration, and solution pH have great effects on Hg^0 removal. Hg^0, and SO_2 concentrations, solution temperature, Fe^{3+}, Cu^{2+}, CO_3^{2-}, and HCO_3^- concentrations also have significant effects on Hg^0 removal. However, concentrations of CO_2, NO, O_2, Cl^-, NO_3^-, SO_4^{2-}, SiO_2, Al_2O_3, and Fe_2O_3 only have slight effects on Hg^0 removal. Hg^0/NO/SO_2 can be simultaneously removed by Photo-Fenton-Like reactions. ·OH was captured, and $SO_4^{2-}/NO_3^-/Hg^{2+}$ were also detected. Removals of Hg^0 by photochemical oxidation and ·OH oxidation play a major role, and removal of Hg^0 by H_2O_2 oxidation only plays a secondary role in removal of Hg^0. © 2015 American Institute of Chemical Engineers *AIChE J*, 61: 1322–1333, 2015
Keywords: Hg^0 removal, photo-Fenton-like reactions, flue gas, simultaneous removal of Hg^0, NO, and SO_2

Introduction

Mercury has great harm for human health and environment because of its persistence, bioaccumulation, and neurological toxicity.[1,2] Coal combustion is considered as the largest source of anthropogenic mercury emission.[1,2] Mercury in coal-fired flue gas often can be divided into three types: elemental mercury (Hg^0), divalent mercury (Hg^{2+}), and particulate mercury (Hg^p).[3,4] Both Hg^{2+} and Hg^p can be effectively captured by traditional dedusting systems and wet flue gas desulfurization systems. However, due to the low solubility in water and the high volatility at room temperature, Hg^0 is very difficult to remove by traditional desulfurization and dedusting systems.[3,4] Once Hg^0 enters the atmosphere, it will result in the global mercury pollution through atmospheric transportation.[1,2] Therefore, studying and developing effective Hg^0 removal technologies has become one of the hot topics in the field of flue gas purification.

Related studies show that wet scrubbing and adsorption are the most promising mercury removal technologies.[3,4] Both Hg^{2+} and Hg^0 can be adsorbed by activated carbon or other adsorbents, and then are converted to particulate mercury, which can be captured by traditional dedusting equipments.[5,6] Unfortunately, however, activated carbon has excellent adsorption performance for Hg^0, but the very high cost hinders its large-scale application.[5,6] Some other new adsorbents have shown potential prospects, but because of the deficiencies in high costs and adsorbent's stability and reliability, they are still unable to obtain commercial applications.[5,6] Using wet oxidation technologies such as $KMnO_4$, $K_2S_2O_8$, $NaClO_2$, H_2O_2, Fenton, UV/H_2O_2[3–11], and dry oxidation technologies such as plasma oxidation, ozonation, photocatalytic oxidation, and photochemical oxidation[1,12–17] can effectively remove Hg^0 from flue gas. However, so far, some problems such as secondary pollution of reaction products, application costs, and safety, and reliability, cannot be effectively solved yet, which hinder the industrial application of these technologies.[18]

Due to having very strong oxidizing, environment-friendly features and simple process, homogeneous Photo-Fenton-Like reactions have been widely studied and applied in degrading organic pollutants from industrial wastewater.[19,20] The results of Liu et al. show that Photo-Fenton-Like reactions can oxidize SO_2 and NO_x from flue gas into available sulfuric acid and nitric acid.[21,22] In these works, the related process parameters were optimized, and the reaction mechanism and kinetics were also investigated.[21,22] However, so far, removal of Hg^0 from flue gas using Photo-Fenton-Like

---

Correspondence concerning this article should be addressed to Y. X. Liu at liuyx1984@126.com.

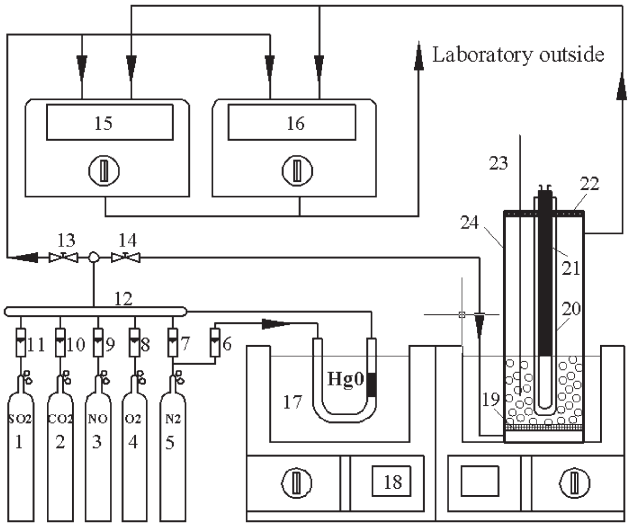

Figure 1. Schematic diagram of experimental device.

(1–5) SO_2, CO_2, NO, O_2, and N_2 cylinders; (6–11) rotameters; (12) gas mixing tank; (13,14) gas valves; (15) flue gas analyzer; (16) flue gas Hg^0 analyzer; (17) Hg^0 generator; (18) constant temperature water bath; (19) sand core gas distribution plate; (20) guartz tube; (21) UV lamp; (22) reactor cover 22; (23) thermometer; and (24) photochemical reactor.

reactions is not reported yet. If Photo-Fenton-Like reactions also can effectively remove Hg^0 in flue gas, it is expected that it may eventually be developed into an effective simultaneous removal technology of SO_2, NO_x, and Hg^0 from flue gas. In this article, removal process of Hg^0 from flue gas by homogeneous Photo-Fenton-Like reactions was investigated in a photochemical reactor. The effects of process parameters, flue gas components, inorganic anions and metal oxides on Hg^0 removal were studied. The active radical was captured and the reaction products were analyzed. Removal pathways of Hg^0 were discussed. Simultaneous removal of Hg^0, NO, and SO_2 with and without additives is also studied preliminarily. The results will provide some theoretical guidance for the industrial applications of this technology.

Experimental Section

Experimental device

It can be seen in Figure 1, the experimental device mainly consists of gas preparation system, detection system and photochemical reactor. Cylinder gases (1–5), including SO_2, CO_2, O_2, NO, and N_2 (Purity, 99.99%), are used to make simulated flue gas and carrier gas. Rotameters (6–11) are used to adjust the flows of gases and the concentrations of gas components. Gas mixing tank (12) is used to strengthen the mixture of five gases. Gas valves (13,14) are used to change the flow direction of simulated flue gas. Flue gas analyzer (15) (MRU-VARIO PLUS, Germany) and flue gas Hg^0 analyzer (16) (QM201H, Suzhou Qingan Instrument Co., China) are used to determinate concentrations of SO_2, CO_2, NO, O_2, and Hg^0, respectively. Hg^0 vapor generator (17) (VICI Metronics) is used to produce Hg^0 vapor. Constant temperature water bath (18) and thermometer (23) are used to adjust solution temperature. The photochemical reactor (24) (High, 36 cm; Inside diameter, 9.0cm) is made of Silicate Glass. Sand core gas distribution plate (19) is installed at 6 cm away from the bottom of photochemical reactor to distribute gas. UV lamp (21) with quartz tube (20) is placed in the center of photochemical reactor to provide excitation light source for photochemical reaction. The solution can be added to the photochemical reactor by opening the reactor cover (22).

Experimental procedures

Before the experiment, 0.4 L Photo-Fenton-Like reagents, including Fe^{3+}/H_2O_2 or Cu^{2+}/H_2O_2, were prepared by H_2O_2/$FeCl_3 \cdot 6H_2O$ and $H_2O_2/CuCl_2 \cdot 2H_2O$ reagents (Guoyao Chemical Reagent Co., AR, China) and deionized water, respectively. The two Photo-Fenton-Like solutions prepared were added to the photochemical reactor by opening the reactor cover, respectively. 2 L/min simulated flue gas was prepared by the cylinder gases and Hg^0 vapor generator. Flows and concentrations of simulated flue gas were regulated by the rotameters. Inlet concentrations of SO_2, CO_2, NO, O_2, and Hg^0 were measured by the flue gas analyzer and flue gas Hg^0 analyzer. Solution temperatures were adjusted to the required values by the constant temperature water bath and the thermometer. When solution temperature reached the required value, turning on the UV lamp, and meanwhile, simulated flue gas began to enter the photochemical reactor to make a gas-liquid reaction by switching gas valves. The outlet concentrations of pollutants were measured by the flue gas analyzer and the flue gas Hg^0 analyzer. Each experimental run was kept for 16 min, and the average concentration within 16 min was used as outlet concentrations of pollutants. The containing-pollutants simulated flue gas was further purified and was discharged to laboratory outside.

Analytical methods

The flue gas Hg^0 analyzer takes a cycle measurement mode of 1 min sampling-3 min measurement-4 min cleaning (Gold amalgamation method is used to capture Hg^0 and fluorescence spectroscopy method is used to measure Hg^0), thus obtaining a value often requires 8 min. The average concentration within 16 min can be obtained by taking the average value of two instantaneous values in the eighth min and the sixteenth min. Before the experiment, 80.0 $\mu g/m^3$ of Hg^0 standard sample was used to test the repeatability of flue gas Hg^0 analyzer, and the results indicated that four measured values were 79.9, 80.0, 80.1, and 80.1 $\mu g/m^3$, respectively (Standard deviation is 0.1 and maximum error is 0.125%.), which showed that the flue gas Hg^0 analyzer had a good repeatability. The SO_2, NO, and O_2 concentrations were measured by electrochemical methods and the CO_2 concentration was measured by nondispersive infrared methods. The related tests about systematical error can be found in Table 2 in the back Section Repeatability Test. To study removal pathways and reaction products of Hg^0 removal, the concentrations of NO_2^-, NO_3^-, SO_3^{2-}, SO_4^{2-}, total mercury, and Hg^0 in solution were measured by ion chromatography (IC) and liquid fluorescence mercury analyzer. The key active intermediate, ·OH, was also captured by electron spin resonance spectrometer (ESR spectrometer, Bruker ESP-300) combining with 5,5-dimethy l-1- pyrrolidine N-oxide (DMPO) (>99%, Sigma) as a spin trap agent. The measurement method of concentrations of total mercury and Hg^0 references the literature.[3]

Removal efficiency

The concentrations of pollutants measured by the gas bypass line are used as the inlet concentration of pollutants.

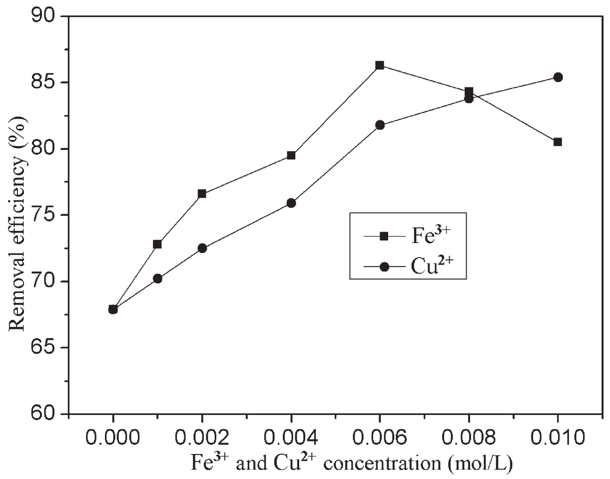

Figure 2. Effects of Fe^{3+} and Cu^{2+} concentrations on Hg^0 removal efficiency.

Conditions: Hg^0 concentration, 30 μg/m^3; CO_2 concentration, 12.0%; O_2 concentration, 6.0%; SO_2 concentration, 800 ppm; NO concentration, 400 ppm; Solution temperature, 318 K; Solution pH value, 3.4; H_2O_2 concentration, 0.40 mol/L; Light wavelength, 254 nm; UV power per unit solution, 0.015 W/mL.

The average concentrations within 16 min measured by the reactor outlet are used as the outlet concentrations of pollutants. The removal efficiency is calculated by the following Eq. 1

$$\text{Removal efficiency } (\%) = \frac{C_{\text{in}} - C_{\text{out}}}{C_{\text{in}}} \times 100\% \tag{1}$$

where C_{in} is the inlet concentration of pollutants in gas; C_{out} is the outlet concentration of pollutants in gas.

Results and Discussions

Effects of Fe^{3+} and Cu^{2+} concentrations

In the Sections Effects of Fe^{3+} and Cu^{2+} Concentration–Simultaneous Removal of Hg^0, NO, and SO_2 Without or with Additives, when a parameter is studied, the other parameters remain unchanged. The related experimental conditions can be found below the Figure captions. Figure 2 shows the effects of Fe^{3+} and Cu^{2+} concentrations on removal efficiency of Hg^0 when the UV lamp is turned on. It can be observed from the Figure 2 that when the other parameters remain unchanged, with Cu^{2+} concentration increasing from 0 to 0.01 mol/L, Hg^0 removal efficiency increases from 67.9 to 85.4%. With Fe^{3+} concentration increasing from 0 to 0.006 mol/L, Hg^0 removal efficiency increases from 67.9 to 86.3%. However, when Fe^{3+} concentration further increases from 0.006 to 0.01 mol/L, Hg^0 removal efficiency decreases from 86.3 to 80.5%. Related results show that Hg^0 from flue gas can be oxidized to Hg^{2+} by ·OH according to the following reaction (2)[3,4]

$$Hg^0 + 2 \cdot OH \rightarrow Hg(OH)_2 \xrightarrow{UV} HgO + H_2O \tag{2}$$

The results[19–22] show that increasing Fe^{3+} and Cu^{2+} concentrations can increase ·OH yields of Photo-Fenton -Like systems by the following reactions (3–10), thereby being able to promote removal of Hg^0

$$Cu^{2+} + H_2O_2 \rightarrow [Cu(HO_2)]^+ + H^+ \tag{3}$$

$$[Cu(HO_2)]^+ \rightarrow Cu^+ + HO_2\cdot \tag{4}$$

$$[Cu(HO_2)]^+ \xrightarrow{UV} Cu^+ + HO_2\cdot \tag{5}$$

$$Cu^+ + H_2O_2 \rightarrow Cu^{2+} + \cdot OH + OH^- \tag{6}$$

$$Fe^{3+} + H_2O_2 \rightarrow [Fe(HO_2)]^{2+} + H^+ \tag{7}$$

$$[Fe(HO_2)]^{2+} \rightarrow Fe^{2+} + HO_2\cdot \tag{8}$$

$$[Fe(HO_2)]^{2+} \xrightarrow{UV} Fe^{2+} + HO_2\cdot \tag{9}$$

$$Fe^{2+} + H_2O_2 \rightarrow Fe^{3+} + \cdot OH + OH^- \tag{10}$$

However, adding excessive Fe^{3+} may result in a consumption of ·OH and H_2O_2 by the following side reactions (11)–(15) with large reaction rates,[19–22] thereby inhibiting removal of Hg^0

$$Fe^{2+} + \cdot OH \rightarrow Fe^{3+} + OH^- \quad k = 3.0 \times 10^8 M^{-1}s^{-1} \tag{11}$$

$$\cdot OH + \cdot OH \rightarrow H_2O_2 \quad k = 5.0 \times 10^9 M^{-1}s^{-1} \tag{12}$$

$$\cdot OH + H_2O_2 \rightarrow H_2O + HO_2\cdot \quad k = 2.7 \times 10^7 M^{-1}s^{-1} \tag{13}$$

$$\cdot OH + HO_2\cdot \rightarrow H_2O + O_2 \quad k = 1.0 \times 10^{10} M^{-1}s^{-1} \tag{14}$$

$$HO_2\cdot + HO_2\cdot \rightarrow H_2O_2 + O_2 \quad k = 3.4 \times 10^7 M^{-1}s^{-1} \tag{15}$$

Thus under the test conditions, when Fe^{3+} concentration exceeds 0.006 mol/L, Hg^0 removal efficiency decreases.

Effects of H_2O_2 concentrations

The effects of H_2O_2 concentration on Hg^0 removal efficiency were studied when the other parameters remain constant, and the results are shown in Figure 3. It can be seen from the Figure 3 that under catalysis of Fe^{3+}, when H_2O_2 concentration increases from 0 to 0.8 mol/L and then further increases from 0.8 to 2.0 mol/L, Hg^0 removal efficiency increases from 52.8 to 89.1% and then decreases from 89.1 to 71.1%, respectively. But under catalysis of Cu^{2+}, when H_2O_2 concentration increases from 0 to 0.4 mol/L and then further increases from 0.4 to 2.0 mol/L, Hg^0 removal efficiency increases from 52.8 to 81.8% and then decreases from 81.8 to 66.3%, respectively. Related results show that 1 mol of H_2O_2 can produce 2 mol of ·OH by the following H_2O_2 photolysis reaction (16).[3,4] ·OH can oxidize and remove Hg^0 from flue gas according to the above reaction (2). It can be inferred from the reaction (16) that in the range of low concentration, the increase of H_2O_2 concentration will increase the yield of ·OH, thereby being able to enhance removal of Hg^0.

$$H_2O_2 \xrightarrow{UV} 2 \cdot OH \tag{16}$$

However, some results[3,4] also show that H_2O_2 is also a scavenger of ·OH, and can consume ·OH by the above side reaction (13) with a very high reaction rate. The oxidizing of the product $HO_2\cdot$ is much weaker than that of ·OH. Thus adding high concentration of H_2O_2 will result in a loss of ·OH and H_2O_2, which can reduce Hg^0 removal efficiency.

In addition, to further study the effects of H_2O_2 concentration, a comparative study on the yield of ·OH in H_2O_2 solution with different concentrations was carried out preliminarily, and the results are shown in Figure 12c–e. It

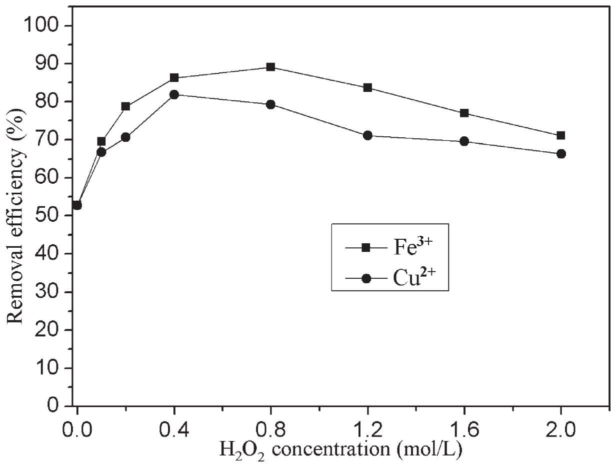

Figure 3. Effects of H_2O_2 concentration on Hg^0 removal efficiency.

Conditions: Hg^0 concentration, 30 μg/m^3; CO_2 concentration, 12.0%; O_2 concentration, 6.0%; SO_2 concentration, 800 ppm; NO concentration, 400 ppm; Solution temperature, 318 K; Solution pH value, 3.4; Fe^{3+} or Cu^{2+} concentrations, 0.006 mol/L; Light wavelength, 254 nm; UV power per unit solution, 0.015 W/mL.

can be seen in the Figure 12c–e, under catalysis of Cu^{2+}, ESR spectrometer captures clear signals of ·OH in H_2O_2 solution with different concentrations. Compared with 0.1 mol/L (low concentration) and 1.2 mol/L (high concentration) of H_2O_2 solution, 0.4 mol/L H_2O_2 solution (optimized concentration) obtains the highest yield or concentration of ·OH (the yield or concentration of radical is proportional to the peak intensity under the same test conditions.). The measurement results maintain a good consistency with the above discussions.

Effects of light wavelength

Figure 4 shows Hg^0 removal efficiencies in several reaction systems with different wavelengths and ions. It can be seen that when the other parameters remain unchanged, under catalysis of Fe^{3+} and Cu^{2+}, Hg^0 removal efficiencies reach 56.8%/86.3%/49.2%/27.5% (Fe^{3+}) and 54.5%/81.8%/40.8%/18.8% (Cu^{2+}) under 185, 254, 365 nm, and visible light, respectively. It is well known that the energy of an ultraviolet photon can be calculated by the following Planck Eq. 17[3,4]

$$\varepsilon = hv = h\frac{c}{\lambda} \tag{17}$$

where ε- energy of photon, J; v- ultraviolet frequency, 1/s; *h*- Planck constant, 6.626 × 10^{-34} J·s; *c*-speed of light, 2.998 × 10^8 m/s; and λ- ultraviolet wavelength, 100–380 nm.

It can be inferred from the above Planck Eq. 17 that when ultraviolet light wavelength becomes shorter, the energy of ultraviolet light photon will become higher. A higher ultraviolet light photon energy can more fully destroy the peroxide bond in H_2O_2 and therefore produce more ·OH radicals. However, when ultraviolet light wavelength becomes shorter, the propagation distance of ultraviolet light in solution also will become shorter due to the heat dissipation characteristics of ultraviolet light propagation in mediums. Synthetically considering the propagation distance and the ultraviolet light photon energy, 254 nm is the most effective ultraviolet light wavelength in the present photochemical reaction system, and achieves the highest Hg^0 removal efficiency. In addition, Granite and Pennline et al. also found 254 nm ultraviolet light to be highly effective in removing mercury from flue gas,[14,16,17] which maintains consistency with the present results.

Effects of UV power per unit solution

The experiment was conducted to evaluate the effects of UV power per unit solution on Hg^0 removal efficiency (The other parameters remain constant). It can be seen from Figure 5 that when UV power per unit solution increases from 0 to 0.025 W/mL, Hg^0 removal efficiency greatly increases from 27.5 to 89.5% and from 18.8 to 82.9% under catalysis of Fe^{3+} and Cu^{2+}, respectively. According to the above photolysis reaction (16), with the increase of UV power per unit solution, the ultraviolet light photon will become more numerous, and then the yield of ·OH also will increase, thereby being able to increase Hg^0 removal efficiency. In addition, the results of Granite et al. show that in any radiation process, the parasitic power or energy consumption is typically the major operating expense.[14–17] Thus choosing a reasonable UV power per unit solution should fully consider the energy consumption and the remove efficiency. The initial results in Figure 5 will help further determine the parasitic power needed for the process in the future works.

Effects of solution pH value

The effects of solution pH value on Hg^0 removal efficiency was studied when the other parameters remain unchanged. From the Figure 6, it can be seen that when solution pH value increases from 1.2 to 11.2, Hg^0 removal efficiency greatly decreases from 94.5 to 32.2% and from 87.8 to 35.5% under catalysis of Fe^{3+} and Cu^{2+}, respectively. Related results show that H_2O_2 in alkaline solution can produce HO_2^- to consume ·OH and H_2O_2 by the following reactions (18) and (19)[3,4,20,22]

$$H_2O_2 \leftrightarrow HO_2^- + H^+ \tag{18}$$

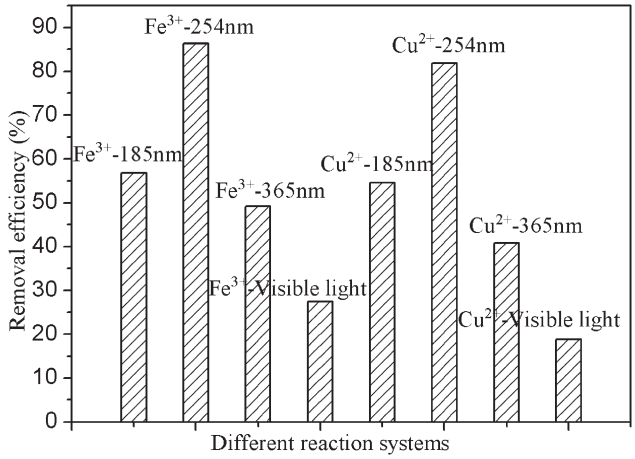

Figure 4. Hg^0 removal efficiencies in several reaction systems with different wavelengths and ions.

Conditions: Hg^0 concentration, 30 μg/m^3; CO_2 concentration, 12.0%; O_2 concentration, 6.0%; SO_2 concentration, 800 ppm; NO concentration, 400 ppm; Solution temperature, 318 K; Solution pH value, 3.4; Fe^{3+} or Cu^{2+} concentrations, 0.006 mol/L; H_2O_2 concentration, 0.40 mol/L; UV power per unit solution, 0.015 W/mL.

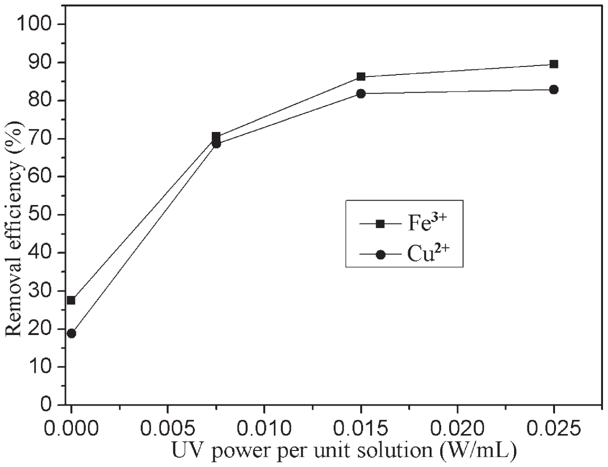

Figure 5. Effects of UV power per unit solution on Hg^0 removal efficiency.

Conditions: Hg^0 concentration, 30 μg/m^3; CO_2 concentration, 12.0%; O_2 concentration, 6.0%; SO_2 concentration, 800 ppm; NO concentration, 400 ppm; Solution temperature, 318 K; Solution pH value, 3.4; Fe^{3+} or Cu^{2+} concentrations, 0.006 mol/L; H_2O_2 concentration, 0.40 mol/L; Light wavelength, 254 nm.

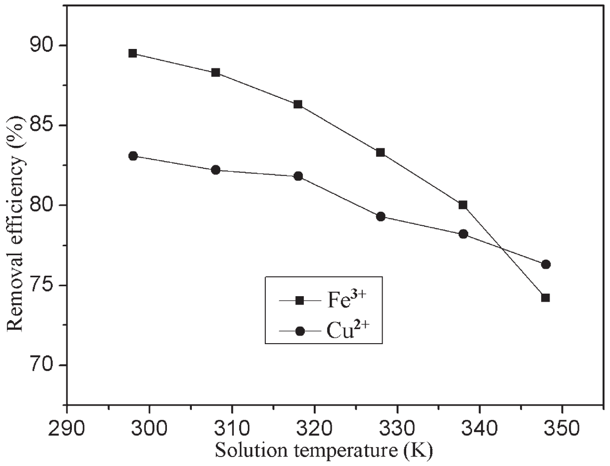

Figure 7. Effects of solution temperature on Hg^0 removal efficiency.

Conditions: Hg^0 concentration, 30 μg/m^3; CO_2 concentration, 12.0%; O_2 concentration, 6.0%; SO_2 concentration, 800 ppm; NO concentration, 400 ppm; Solution pH value, 3.4; Fe^{3+} or Cu^{2+} concentrations, 0.006 mol/L; H_2O_2 concentration, 0.40 mol/L; Light wavelength, 254 nm; UV power per unit solution, 0.015 W/mL.

$$\cdot OH + HO_2^- \rightarrow H_2O + O_2^- \cdot \tag{19}$$

It can be seen from the above reactions (18) and (19) that increasing solution pH value can increase OH^- concentration to neutralize H^+, which can further increase the yield of HO_2^-.[20] Besides, some results show that H_2O_2 and Photo-Fenton-Like reagents often have weaker oxidizing under alkaline conditions as compared to acidic conditions.[19–22] Therefore, under these test conditions, with the increase of solution pH value, Hg^0 removal efficiency has a large decrease.

Effects of solution temperature

The effects of solution temperature on Hg^0 removal efficiency were studied when the other parameters keep constant, and the results are shown in Figure 7. It can be seen that when solution temperature increases from 298 to 348 K, Hg^0 removal efficiency decreases from 89.5 to 74.2% and from 83.1 to 76.3% under catalysis of Fe^{3+} and Cu^{2+}, respectively. According to the Arrhenius equation, increasing solution temperature will increase the chemical reaction rate,[20] thereby promoting removal of Hg^0. However, increasing solution temperature also will reduce the solubility of Hg^0 in water [the solubilities of Hg^0 in water are 112.0 × 10^{-3} (298 K), 67.4 × 10^{-3} (308 K), 42.4 × 10^{-3} (318 K), 28.0 × 10^{-3} (328 K), 19.3 × 10^{-3} (338 K), and 13.6 × 10^{-3} (348 K) kmol/(m^3·atm)],[9,23] thereby weakening Hg^0 removal. In this article, with the increase of solution temperature, the reduction of Hg^0 solubility may play a major role, which eventually results in the decrease of Hg^0 removal efficiency.

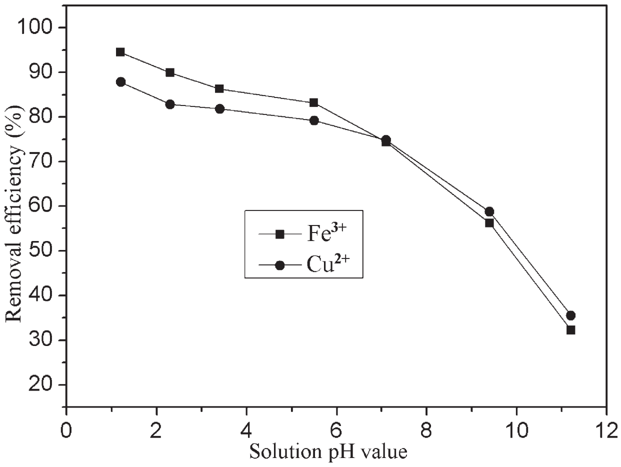

Figure 6. Effects of solution pH value on Hg^0 removal efficiency.

Conditions: Hg^0 concentration, 30 μg/m^3; CO_2 concentration, 12.0%; O_2 concentration, 6.0%; SO_2 concentration, 800 ppm; NO concentration, 400 ppm; Solution temperature, 318 K; Fe^{3+} or Cu^{2+} concentrations, 0.006 mol/L; H_2O_2 concentration, 0.40 mol/L; Light wavelength, 254 nm; UV power per unit solution, 0.015 W/mL.

Effects of Hg^0 concentration

The effects of Hg^0 concentration on Hg^0 removal efficiency was studied when the other parameters remain unchanged, and the results are shown in Figure 8. As shown in Figure 8, under catalysis of Fe^{3+}, when Hg^0 concentration increases from 10 to 30 μg/m^3 and then further increases from 30 to 50 μg/m^3, Hg^0 removal efficiency increases from 81.1 to 86.1% and then almost keeps constant. But under catalysis of Cu^{2+}, when Hg^0 concentration increases from 10 to 50 μg/m^3, Hg^0 removal efficiency continuously decreases from 83.2 to 77.1%. According to the two-film theory, Hg^0 absorption rate can meet the following Eq. 20[3,4,23]

$$N_{Hg^0} = k_{Hg^0,G}(p_{Hg^0,G} - p_{Hg^0,i}) \tag{20}$$

where N_{Hg^0} is the absorption rate of Hg^0, mol/m$^2 \cdot$ s; $k_{Hg^0,G}$ is the gas-phase mass-transfer coefficient, mol/s $\cdot$ m$^2 \cdot$ Pa; $p_{Hg^0,G}$ is the Hg^0 partial pressure in gas-phase body, Pa; $p_{Hg^0,i}$ is the Hg^0 partial pressure in phase interface, Pa.

From the above Eq. 20, it can be seen that increasing Hg^0 concentration in gas can increase Hg^0 absorption rate by increasing the mass-transfer driving force of Hg^0, which is conducive to removal of Hg^0. When the other test conditions

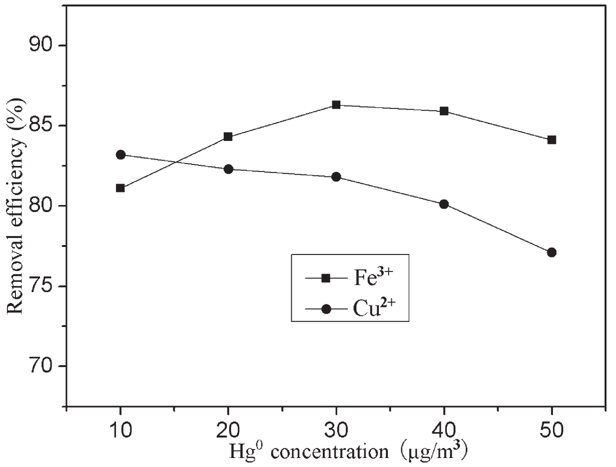

Figure 8. Effects of Hg^0 concentration on Hg^0 removal efficiency.

Conditions: CO$_2$ concentration, 12.0 %; O$_2$ concentration, 6.0 %; SO$_2$ concentration, 800 ppm; NO concentration, 400 ppm; Solution temperature, 318 K; Solution pH value, 3.4; Fe^{3+} or Cu^{2+} concentrations, 0.006 mol/L; H$_2$O$_2$ concentration, 0.40 mol/L; Light wavelength, 254 nm; UV power per unit solution, 0.015 W/mL.

keep constant, the concentrations of ·OH/H$_2$O$_2$/*hv*/H$_2$O also will keep unchanged. But the increase of Hg^0 concentration will increase the number of Hg^0 molecules through reactor per unit time, which will decrease the relative molar ratio of ·OH/H$_2$O$_2$/*hv*/H$_2$O to Hg^0 (the relative molar ratio is defined as [·OH/H$_2$O$_2$/*hv*/H$_2$O concentrations]/[Hg^0 concentration]), thereby being not conducive to removal of Hg^0. It can be inferred from the above experimental results that under catalysis of Fe^{3+}, the front positive factor plays a major role when Hg^0 concentration is located between 10 and 30 μg/m^3. In contrast, the back negative factor plays a major role when Hg^0 concentration is located between 30 and 50 μg/m^3. However, under catalysis of Cu^{2+}, the back negative factor always plays a leading role throughout the range of Hg^0 concentrations (10–50 μg/m^3), and as a result, Hg^0 removal efficiency maintains a monotonic decrease.

Effects of flue gas components

Figure 9 shows the effects of flue gas components (SO$_2$ concentration, CO$_2$ concentration, NO concentration, and O$_2$ concentration) on Hg^0 removal efficiency. It can be seen from Figure 9 that when the other parameters remain unchanged, under catalysis of Fe^{3+} and Cu^{2+}, with the increase of SO$_2$ concentration, Hg^0 removal efficiency slightly decreases. Related results show that SO$_2$ can consume H$_2$O$_2$ and ·OH by the following reactions (21)–(26),[3,4,21,22] thereby weakening Hg^0 removal

$$SO_2 + H_2O \leftrightarrow HSO_3^- + H^+ \tag{21}$$

$$HSO_3^- \leftrightarrow SO_3^{2-} + H^+ \tag{22}$$

$$HSO_3^- + \cdot OH \rightarrow SO_3^- \cdot + H_2O \tag{23}$$

$$SO_3^{2-} + \cdot OH \rightarrow \cdot SO_3^- + OH^- \tag{24}$$

$$HSO_3^- + H_2O_2 \rightarrow SO_4^{2-} + H^+ + H_2O \tag{25}$$

$$SO_3^{2-} + H_2O_2 \rightarrow SO_4^{2-} + H_2O \tag{26}$$

With the increase of NO concentration, Hg^0 removal efficiency very slightly decreases, and the change is not obvious. Related results show that NO also can consume H$_2$O$_2$ and ·OH by the following reactions (27)–(31),[3,4,21,22] thereby weakening Hg^0 removal

$$NO + \cdot OH \rightarrow HNO_2 \tag{27}$$

$$HNO_2 + H_2O_2 \rightarrow HNO_3 + H_2O \tag{28}$$

$$NO_2 + \cdot OH \rightarrow HNO_3 \tag{29}$$

$$2NO_2 + H_2O_2 \rightarrow 2HNO_3 \tag{30}$$

$$2NO + 3H_2O_2 \rightarrow 2HNO_3 + 2H_2O \tag{31}$$

With the increase of O$_2$ concentration, Hg^0 removal efficiency only very slightly increases, but the change is also not obvious. Related results show that O$_2$ often can play an important role in hindering the collisions and destruction of free radicals by the following chain reactions (32) and (33).[3,4,22,24] It can be seen that ·OH is consumed by the reaction (32), and then is regenerated by the reaction (33), which can effectively restrain the above side reactions (11)–(14), then increasing the effective utilization of ·OH

$$O_2 + \cdot OH \rightarrow HO_2 \cdot + \cdot O \quad k = 10^8 - 10^{12} M^{-1} s^{-1} \tag{32}$$

$$H_2O_2 + \cdot O \rightarrow HO_2 \cdot + \cdot OH \quad k = 1.6 \times 10^9 M^{-1} s^{-1} \tag{33}$$

Therefore, under the test conditions, the increase of O$_2$ concentration can slightly improve removal of Hg^0. Because the stable valences of C and O in CO$_2$, CO$_2$ is generally considered to be a low-active substance in the oxidation-reduction reactions. Therefore, under the test conditions, with the increase of CO$_2$ concentration, Hg^0 removal efficiency almost has no change. The above results show that the change of flue gas components concentrations only has a small impact on Hg^0 removal, which demonstrates that Hg^0 removals by homogeneous Photo-Fenton-Like reactions have a good adaptability for the changes of flue gas components.

Effects of inorganic anions and metal oxides

Effects of NO$_3^-$, Cl$^-$, and SO$_4^{2-}$. It is well known that inorganic ions and metal oxides are widely present in natural waters or coal-fired flue gases. Thus it is very necessary to study the effects of inorganic ions and metal oxides on removal of Hg^0 from flue gas by homogeneous Photo-Fenton-Like reactions. Figure 10 shows the effects of common inorganic ions and metal oxides (SO$_4^{2-}$, NO$_3^-$, Cl$^-$, CO$_3^{2-}$, HCO$_3^-$, Al$_2$O$_3$, SiO$_2$, and Fe$_2$O$_3$) on Hg^0 removal efficiency. It can be seen in Figure 10a that when the other parameters remain unchanged, the addition of NO$_3^-$ or Cl$^-$ has a slight inhibition for Hg^0 removal, but the addition of SO$_4^{2-}$ has a slight promotion for Hg^0 removal. Related results show that both Cl$^-$ and NO$_3^-$ can react with ·OH to produce NO$_3$· and ·Cl according to the following reactions (34)–(36), which will result in consumption of ·OH.[25–29] The oxidizability of the secondary products, ·Cl and ·NO$_3$ is much weaker than that of ·OH,[26,29] thereby being not conducive to removal of Hg^0

$$Cl^- + \cdot OH \leftrightarrow HOCl^- \cdot \tag{34}$$

$$HOCl^- \cdot + H^+ \leftrightarrow Cl \cdot + H_2O \tag{35}$$

$$NO_3{}^- + \cdot OH \rightarrow \cdot NO_3 + OH^- \tag{36}$$

Unlike NO$_3^-$ and Cl$^-$, SO$_4^{2-}$ also can react with ·OH to produce SO$_4^{2-}$· according to the following reaction (37),[25–29] but the secondary product, SO$_4^{2-}$·, also has a very strong

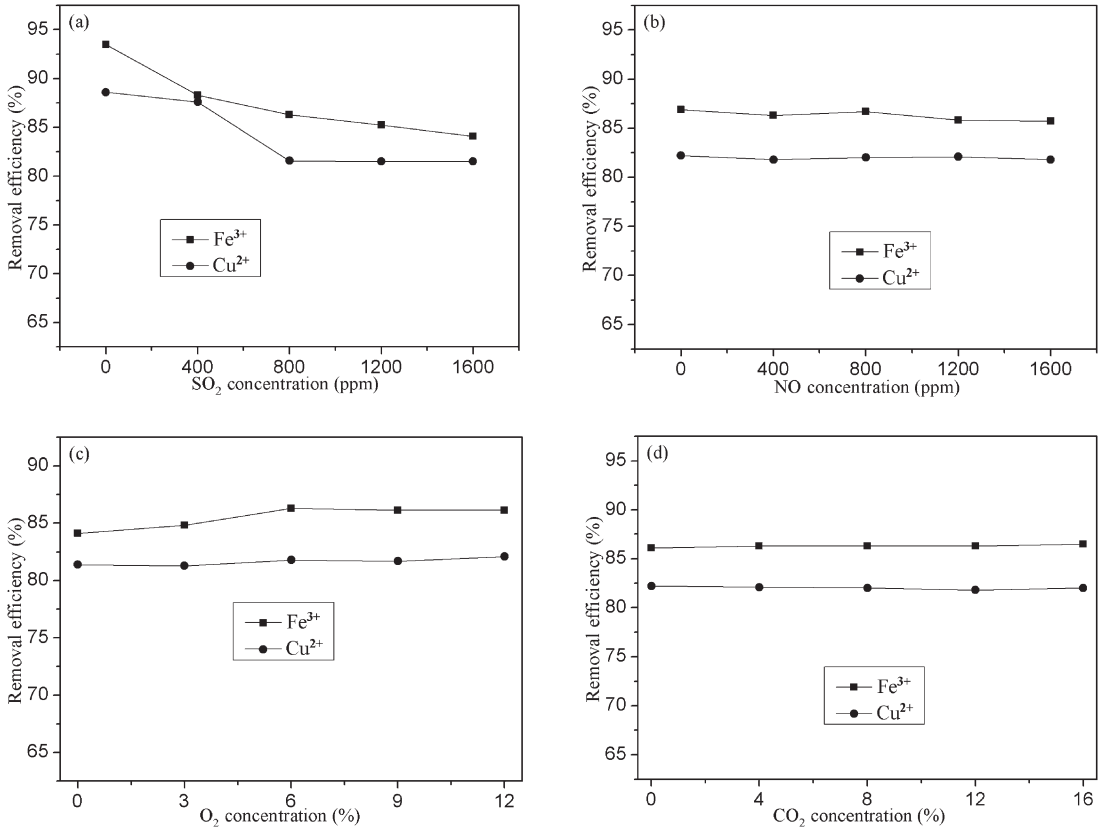

Figure 9. Effects of flue gas components on Hg^0 removal efficiency.

Conditions: Hg^0 concentration, 30 μg/m^3; Solution temperature, 318 K; Solution pH value, 3.4; Fe^{3+} or Cu^{2+} concentrations, 0.006 mol/L; H_2O_2 concentration, 0.40 mol/L; Light wavelength, 254 nm; UV power per unit solution, 0.015 W/mL.

oxidizability, and it can directly oxidize Hg^0 by the following reaction (38)[30]

$$SO_4^{2-} + \cdot OH \rightarrow SO_4^{-}\cdot + OH^{-} \tag{37}$$

$$2SO_4^{-}\cdot + Hg^0 \rightarrow Hg^{2+} + 2SO_4^{2-} \tag{38}$$

Besides, $SO_4^{-}\cdot$ also can react with H_2O to reproduce ·OH by the following reaction (39)[30]

$$SO_4^{-}\cdot + H_2O \rightarrow \cdot OH + HSO_4^{-} \tag{39}$$

It can be seen from the above reactions (37)–(39) that as an intermediate, SO_4^{2-} plays an important role in hindering the destruction of ·OH radicals, thereby being conducive to removal of Hg^0.

Effects of HCO_3^- and CO_3^{2-}. It can be seen from Figure 10a that when the other parameters remain constant, with the additions of HCO_3^- and CO_3^{2-}, Hg^0 removal efficiencies greatly decrease. Related results[25–29] show that as the scavengers of ·OH, both HCO_3^- and CO_3^{2-} can consume ·OH by the following reactions (40) and (41). The oxidizability of the secondary product, CO_3^-, is also much weaker than that of ·OH,[26,29] thereby being not conducive to removal of Hg^0

$$HCO_3^{-} + \cdot OH \rightarrow CO_3^{-}\cdot + H_2O \tag{40}$$

$$CO_3^{2-} + \cdot OH \rightarrow CO_3^{-}\cdot + OH^{-} \tag{41}$$

Besides, both HCO_3^- and CO_3^{2-} can produce OH^- in solution by the following hydrolysis reactions (42) and (43)[31]

$$HCO_3^{-} + H_2O \leftrightarrow H_2CO_3 + OH^{-} \tag{42}$$

$$CO_3^{2-} + H_2O \leftrightarrow HCO_3^{-} + OH^{-} \tag{43}$$

The previous results (Section Effects of Solution pH Value) have shown that increasing solution pH value (or increasing OH^- concentration) can greatly decrease Hg^0 removal efficiency. Therefore, under the test conditions, both HCO_3^- and CO_3^{2-} have significant negative impacts on removal of Hg^0.

Effects of Al_2O_3, SiO_2, and Fe_2O_3. It can be seen from Figure 10b that when the other parameters remain unchanged, with the additions of Al_2O_3, SiO_2, and Fe_2O_3, Hg^0 removal efficiencies decrease. According to the following Beer-Lambert Law Eq. 44,[31] with the increase of medium concentration, UV transmitted light intensity will have an exponential decrease. Al_2O_3, SiO_2, and Fe_2O_3 are particulate matters, thus the addition of Al_2O_3, SiO_2, or Fe_2O_3 will lead to the reflection and scattering of UV light in solution, which is able to diminish the penetration rate of UV light in solution, thereby weakening photochemical reaction of Hg^0

$$I_a = I_0 \exp\left(-klc_B\right) \tag{44}$$

where I_a- UV transmitted light intensity, W/cm^2; I_0- UV incident light intensity, W/cm^2; k- Light absorption coefficient; l- Dielectric layer thickness, cm; and c_B- Medium concentration, mol/L.

In addition, during the experiment, it was found that the addition of Al_2O_3, SiO_2, or Fe_2O_3 apparently aggravated the coalescence of small bubbles in the photochemical reactor. Coalescence of small bubbles will result in the decline of gas-liquid interfacial area, and then can weaken the gas-

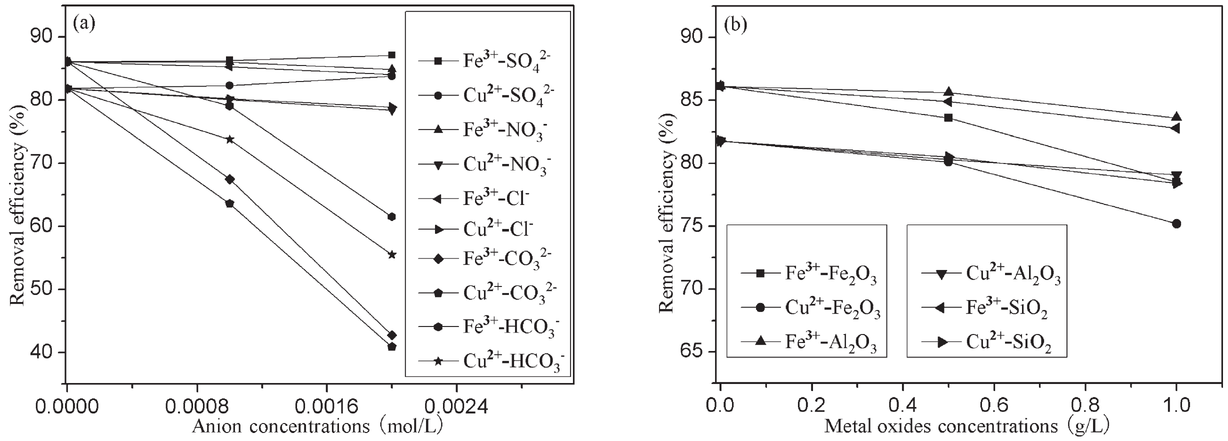

Figure 10. Effects of inorganic anions and metal oxides on Hg^0 removal efficiency.

Conditions: Hg^0 concentration, 30 μg/m^3; CO_2 concentration, 12.0 %; O_2 concentration, 6.0%; SO_2 concentration, 800 ppm; NO concentration, 400 ppm; Solution temperature, 318 K; Solution pH value, 3.4; Fe^{3+} or Cu^{2+} concentrations, 0.006 mol/L; H_2O_2 concentration, 0.40 mol/L; Light wavelength, 254 nm; UV power per unit solution, 0.015 W/mL.

liquid reaction,[23,32] being not conducive to removal of Hg^0. Thus under the test conditions, with the additions of Al_2O_3, SiO_2, and Fe_2O_3, Hg^0 removal efficiencies decrease.

Comparative study

The comparison study in different reaction systems was carried out and the results are shown in Figure 11. It can be seen that under catalysis of Fe^{3+}/Cu^{2+}, Hg^0 can achieve removal efficiencies of 52.8%/52.8%, 7.3%/7.3%, 27.5%/18.8%, 86.3%/81.8%, and 67.9%/67.9% in UV [Column A], H_2O_2 [Column B], Fenton-Like reactions [Column C], Photo-Fenton-Like reactions [Column D], and UV/H_2O_2 [Column E], respectively. The above results show that Photo-Fenton-Like reactions have the best performance for removal of Hg^0 and there are significant synergistic effects among UV, H_2O_2 and Fe^{3+}/Cu^{2+}.

Capture of ·OH radicals

The capture of key radicals in chemical reaction process is a very important work for studying the mechanism and reaction pathways of Hg^0 removal. In the present work, the key ·OH in solution was captured by ESR spectrometer combining with DMPO, and the results are shown in Figure 12. As shown in Figure 12a, ESR spectrometer cannot capture a clear radical signal without adding H_2O_2 (blank sample). However, it can be seen in Figure 12b–e, under catalysis of Fe^{3+} and Cu^{2+}, the typical four-line ESR spectra was detected in H_2O_2 solutions with different concentrations when the UV lamp was turned on, respectively. The hyperfine splitting constants $a_N = 15.2$ G and $a_H = 14.7$ G were in good agreement with the literature data $a_N = 15.0$ G and $a_H = 14.8$ G.[30,32] The results show that ·OH was produced in the two reaction systems. The results can provide powerful supports for verifying the reaction pathway of Hg^0 removal by ·OH oxidation.

Reaction products

To study the reaction pathways of Hg^0 removal, the concentrations of NO_2^-, NO_3^-, SO_3^{2-}, SO_4^{2-}, total mercury, and Hg^0 in solution were measured by IC and fluorescence mercury analyzer, and the results are shown in Table 1. The results show that SO_3^{2-}, NO_2^-, and Hg^0 are not detected in mixed solution. However, SO_4^{2-}, NO_3^-, and Hg^{2+} are detected in mixed solution. The SO_4^{2-} may be the oxidation product of SO_2 from flue gas, and the NO_3^- may be the oxidation product of NO from flue gas. The

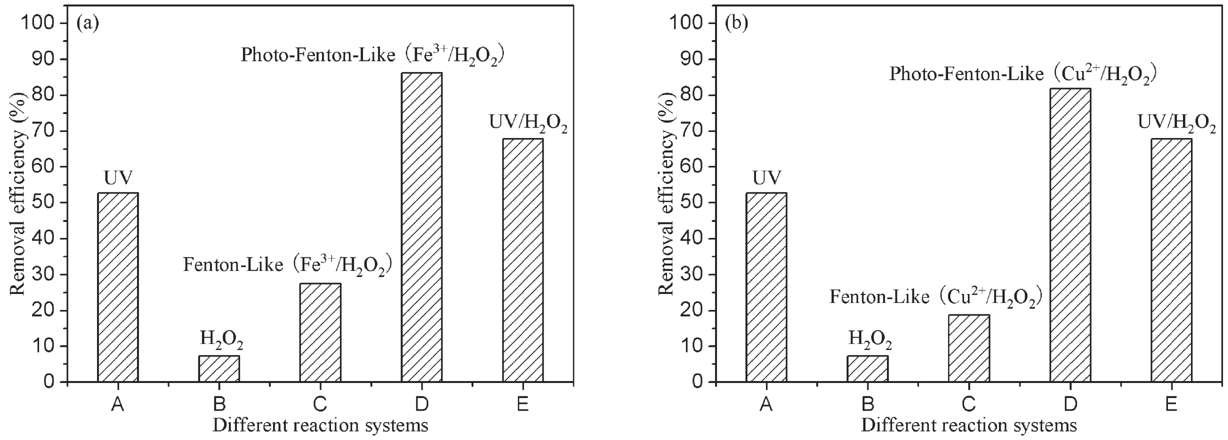

Figure 11. Comparison study in different reaction systems.

Conditions: Hg^0 concentration, 30 μg/m^3; CO_2 concentration, 12.0%; O_2 concentration, 6.0%; SO_2 concentration, 800 ppm; NO concentration, 400 ppm; Solution temperature, 318 K; Solution pH value, 3.4; Fe^{3+} or Cu^{2+} concentrations, 0.006 mol/L; H_2O_2 concentration, 0.40 mol/L; Light wavelength, 254 nm; UV power per unit solution, 0.015 W/mL.

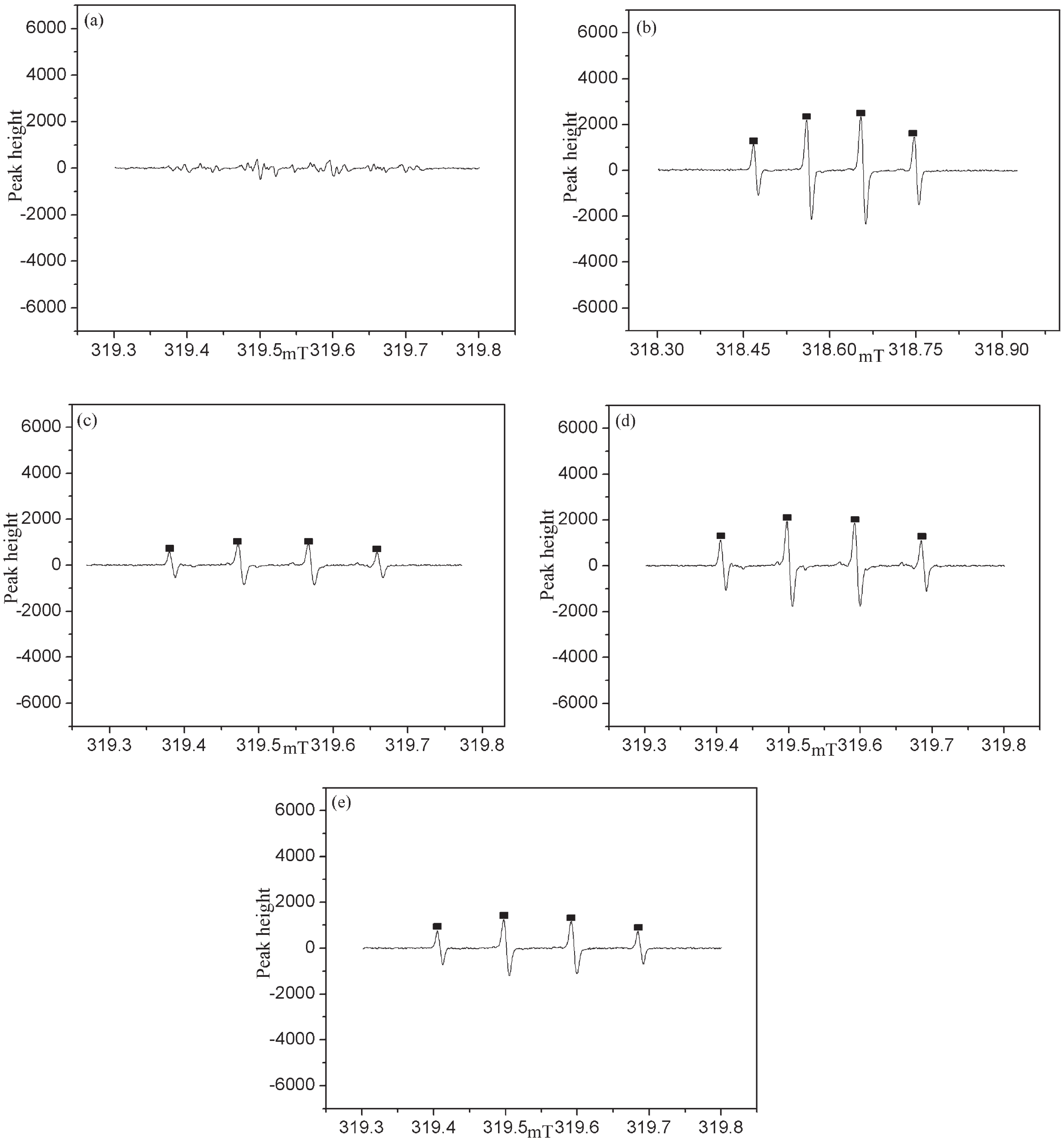

Figure 12. ESR spectrums of ·OH radical adducts.

(a) Blank sample; (b) catalysis of Fe^{3+} in 0.4 mol/L of H_2O_2 solution; (c) catalysis of Cu^{2+} in 0.1 mol/L of H_2O_2 solution; (d) catalysis of Cu^{2+} in 0.4 mol/L of H_2O_2 solution; and (e) catalysis of Cu^{2+} in 1.2 mol/L of H_2O_2 solution.

Hg^{2+} may be the oxidation product of Hg^0 from flue gas. To further verify the transfer pathways of N, S, and Hg in flue gas, based on the results of oxidation product concentrations and removal efficiency, the calculations of mass balances for NO, SO_2 and mercury were carried out and the results are shown in Table 1. It can be seen that the determined values of total N, S and mercury concentrations are in good agreement with the predicted values. The results further suggest that NO, SO_2 and Hg^0 are mainly removed by oxidation reactions, and SO_4^{2-}, NO_3^-, and Hg^{2+} are the main reaction products of NO, SO_2, and Hg^0 removals, respectively.

Table 1. Reaction Products and Mass Balances for NO, SO_2, and Mercury

Ion category (catalysis of Fe^{3+})	SO_4^{2-}	SO_3^{2-}	NO_3^-	NO_2^-	Total mercury	Hg^0
Measured concentration (mg/L)	249.8	0	29.8	0	1.73 (μg/L)	0
Theoretical concentration(mg/L)	274.5	–	34.1	–	2.07 (μg/L)	–
Relative error (%)	8.9%	–	12.6%	–	16.4%	–
Ion category (catalysis of Cu^{2+})	SO_4^{2-}	SO_3^{2-}	NO_3^-	NO_2^-	Total mercury	Hg^0
Measured concentration (mg/L)	263.1	0	25.7	0	1.77 (μg/L)	0
Theoretical concentration(mg/L)	274.5	–	28.0	–	1.96 (μg/L)	–
Relative error (%)	4.2%	–	8.2 %	–	9.0%	–

Table 2. The Repeatability Tests of Hg^0, SO_2, and NO Removal Efficiencies

Under catalysis of Fe^{3+}	No. 1	2	3	4	Average	Standard deviation
Average removal efficiency of Hg^0, (%)	86.2	86.3	86.2	86.4	86.3	0.10
Average removal efficiency of NO, (%)	38.6	38.5	38.5	38.4	38.5	0.08
Average removal efficiency of SO_2, (%)	100	100	100	100	100	0.00

For the after-treatment of the mixed reaction products, the Hg^{2+} in mixed solution can be separated by adding S^{2+} to react with Hg^{2+} to produce HgS precipitation, which can be recycled by simple precipitation separation in a separation tower. The remaining sulfuric acid and nitric acid solution will be used for the manufacture of agricultural fertilizers by adding ammonia to produce ammonium sulfate and ammonium nitrate, which has no secondary pollution. The evaporation and crystallization process of ammonium sulfate and ammonium nitrate can be carried out using waste heat from boiler flue gas (exhaust gas temperature of boilers is typically greater than 120°C), which does not require additional energy consumption.

Reaction pathways

The determined results of ESR spectrometer in Figure 11a show that there is almost no clear radical signal in the reaction system without adding H_2O_2/Fe^{3+} or H_2O_2/Cu^{2+} (or only using UV irradiation), but at this time, Hg^0 removal efficiency still reaches 52.8% (Figure 10), which prove that this part of Hg^0 removal efficiency may come from photochemical oxidation removal of Hg^0 according to the following reaction (45)[3,4]

$$Hg^0 + H_2O + hv \xrightarrow{(\lambda = 254\text{nm})} HgO + H_2 \qquad (45)$$

It can be seen in Figure 10 that Hg^0 removal efficiency is 7.3% using oxidation of H_2O_2 alone, showing that removal of Hg^0 by oxidation of H_2O_2 occurs in the reaction system. The great increase of Hg^0 removal efficiencies in two Photo-Fenton-Like reactions, and the successful capture of ·OH by ESR spectrometer shows that Hg^0 has been removed by oxidation of ·OH. The results of reaction products and mass balance calculations also show that NO, SO_2, and Hg^0 are mainly removed by oxidation reactions, and SO_4^{2-}, NO_3^-, and Hg^{2+} are the main oxidation products, which can further prove that the oxidation reactions above-mentioned have occurred in the reaction process. Besides, based on Hg^0 removal efficiencies in different reaction systems, it can be inferred that removals of Hg^0 by photochemical oxidation and ·OH oxidation play a major role, and removal of Hg^0 by H_2O_2 oxidation only plays a secondary role for removal of Hg^0. In summary, the mechanism and reaction pathways of Hg^0 removal in Photo-Fenton-Like reactions may be described by the following Figure 13.

Simultaneous removal of Hg^0, NO, and SO_2 without or with additives

At present, studying and developing effective simultaneous removal technologies of NO_x, SO_2, and Hg^0 from flue gas has become one of the hot issues in the field of flue gas purification.[32–35] In this work, simultaneous removal of Hg^0, NO, and SO_2 from flue gas by two homogeneous Photo-Fenton-Like reactions was investigated preliminarily in the photochemical reactor, and the results are shown in Figure 14. It can be seen in Figure 14a that NO, SO_2, and Hg^0 can be removed simultaneously, and the simultaneous removal efficiencies of NO, Hg^0 and SO_2 are 38.5, 86.1, and 100% under catalysis of Fe^{3+}, and are 31.3, 81.8, and 100% under catalysis of Cu^{2+}, respectively. The results indicate that Hg^0 and SO_2 can be efficiently removed, but NO can not be efficiently removed because of its very low solubility in water. Therefore, it is very necessary to look for effective measures to strengthen removal of NO.

To strengthen removal of NO by two homogeneous Photo-Fenton-Like reactions, several representative and effective strengthening additives[31,33–35] such as TiO_2 photocatalyst (representing catalysts), $CaCO_3$ (representing alkaline substances) and $Na_2S_2O_8$ (representing peroxides) were added to the photochemical reactor, and the results can be seen in Figure 14b–d. It can be observed that with the increase of TiO_2, $CaCO_3$, or $Na_2S_2O_8$ concentration, SO_2 can still keep 100% removal. However, unlike SO_2, both Hg^0 and NO removal efficiencies significantly change. For example, with the increase of TiO_2 concentration, both Hg^0 and NO removal efficiencies decrease under catalysis of Fe^{3+} and Cu^{2+}. With the increase of $CaCO_3$ concentration, NO removal efficiency greatly increases, but Hg^0 removal efficiency greatly decreases under catalysis of Fe^{3+} and Cu^{2+}. Based on the addition of $CaCO_3$, and with the increase of $Na_2S_2O_8$ concentration, both Hg^0 and NO removal efficiencies obviously increase under catalysis of Fe^{3+} and Cu^{2+}. The results show that both homogeneous Photo-Fenton-Like reactions may be used to simultaneously remove Hg^0, NO, and SO_2 from flue gas with the addition of $CaCO_3$ and $Na_2S_2O_8$. The related contents about simultaneous removal of NO, SO_2 and Hg^0 by combined process will be further studied in the future works.

Repeatability test

The repeatability tests were carried out to evaluate the stability and reliability of the experimental system and

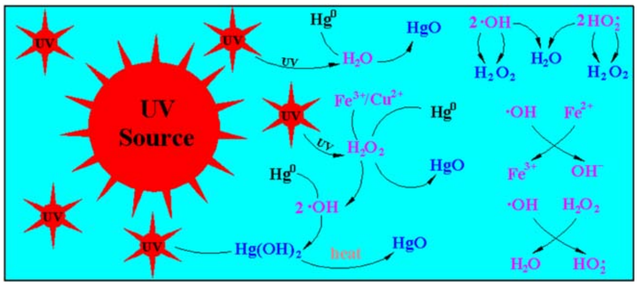

Figure 13. Schematic diagram of mechanism and reaction pathways of Hg^0 removals by two Photo-Fenton-Like reactions.

[Color figure can be viewed in the online issue, which is available at wileyonlinelibrary.com.]

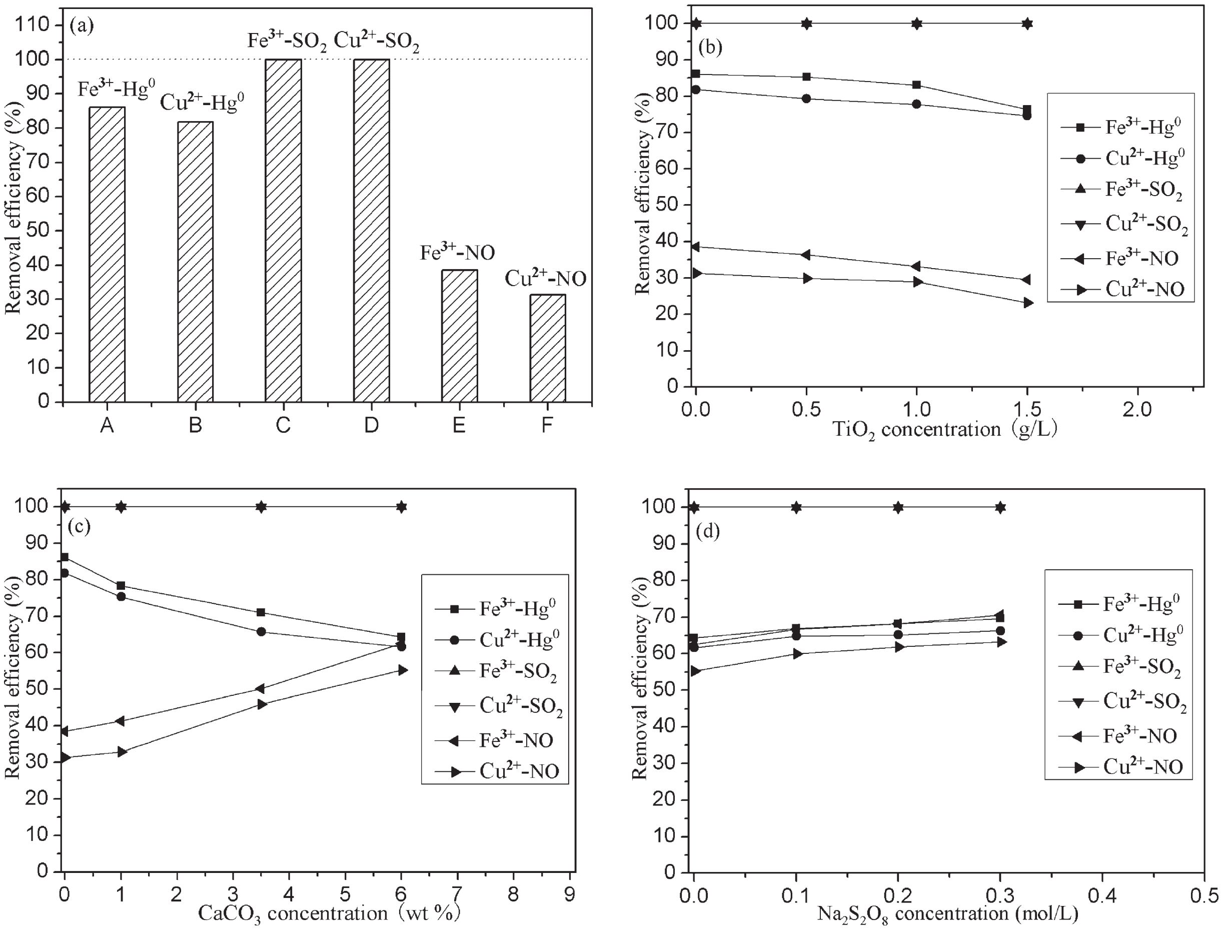

Figure 14. Effects of additive concentrations on simultaneous removal efficiencies of Hg^0, NO, and SO_2.

Conditions: Hg^0 concentration, 30 μg/m^3; CO_2 concentration, 12.0%; O_2 concentration, 6.0%; SO_2 concentration, 800 ppm; NO concentration, 400 ppm; Solution temperature, 318 K; Solution pH value, 3.4; Fe^{3+} or Cu^{2+} concentrations, 0.006 mol/L; H_2O_2 concentration, 0.40 mol/L; Light wavelength, 254 nm; UV power per unit solution, 0.015 W/mL.

measurement method under the following experimental conditions: Hg^0 concentration, 30 μg/m^3; CO_2 concentration, 12.0%; O_2 concentration, 6.0%; SO_2 concentration, 800 ppm; NO concentration, 400 ppm, solution temperature, 318 K, solution pH value, 3.4, Fe^{3+} or Cu^{2+} concentrations, 0.006 mol/L, H_2O_2 concentration, 0.40 mol/L, light wavelength, 254 nm, UV power per unit solution, 0.015 W/mL, and the results are shown in xxTable 2. The results show that Hg^0, SO_2, and NO removal efficiencies have good reproducibility and can provide reliable results.

Conclusions

The main conclusions of this article are as follows: UV power per unit solution, light wavelength, H_2O_2 concentration, and solution pH has great effects on Hg^0 removal. Hg^0 and SO_2 concentrations, solution temperature, Fe^{3+}, Cu^{2+}, CO_3^{2-}, and HCO_3^- concentrations also have significant effects on Hg^0 removal. However, the concentrations of CO_2, NO, O_2, Cl^-, NO_3^-, SO_4^{2-}, SiO_2, Al_2O_3, and Fe_2O_3 only have slight effects on Hg^0 removal. Hg^0, NO, and SO_2 can be simultaneously removed by two homogeneous Photo-Fenton-Like reactions, but NO removal efficiency is low. Simultaneous removal of Hg^0, NO, and SO_2 can be enhanced by simultaneously adding $CaCO_3$ and $Na_2S_2O_8$, but was weakened by adding TiO_2 alone. Photo-Fenton-Like reactions have the best performance for removal of Hg^0 and there are significant synergistic effects among UV, H_2O_2 and Fe^{3+}/Cu^{2+}. The key ·OH in solution were captured by ESR spectrometer combining with DMPO under catalysis of Fe^{3+} or Cu^{2+}. NO, SO_2 and Hg^0 are mainly removed by oxidation reactions, and SO_4^{2-}, NO_3^-, and Hg^{2+} are the main oxidation products. Removals of Hg^0 by photochemical oxidation and ·OH oxidation play a major role, and removal of Hg^0 by H_2O_2 oxidation only plays a secondary role for removal of Hg^0.

Acknowledgments

This study was supported by National Natural Science Foundation of China (No.51206067), National Key Basic Research Program 973 Project of China (No.2013CB228504), Open Research Fund Program of Key Laboratory of Energy Thermal Conversion and Control of Ministry of Education (Southeast University), Key Laboratory of Efficient & Clean Energy Utilization, College of Hunan Province (Changsha University of Science & Technology), Training Project of Jiangsu University Youth Backbone Teacher.

Literature Cited

1. Yang SJ, Yan NQ, Guo YF, Wu DQ, He HQ. Gaseous elemental mercury capture from flue gas using magnetic nanosized (Fe$_3$-xMnx)1-δO4. *Environ Sci Technol*. 2011;45:1540–1546.

2. Byun YC, Koh DJ, Shin DN. Removal mechanism of elemental mercury by using non-thermal plasma. *Chemosphere.* 2011;83:69–75.
3. Liu YX, Pan JF, Wang Q. Removal of Hg^0 from containing-SO_2/NO flue gas by ultraviolet/H_2O_2 process in a novel photochemical reactor. *AIChE J.* 2014;6:2275–2285.
4. Liu YX, Zhang J, Yin YS. Study on absorption of elemental mercury from flue gas by UV/H_2O_2: process parameters and reaction mechanism. *Chem Eng J.* 2014;249:72–78.
5. Granite EJ, Pennline HW, Hargis RA. Novel sorbents for mercury removal from flue gas. *Ind Eng Chem Res.* 2000;39:1020–1029.
6. Granite EJ, Freeman MC, Hargis RA, O'Dowd WJ, Pennline HW. The thief process for mercury removal from flue gas. *J Environ Manage.* 2007;4:628–634.
7. Fang P, Cen CP, Wang XM, Tang ZJ, Tang ZX, Chen DS. Simultaneous removal of SO_2, NO and Hg^0 by wet scrubbing using urea+$KMnO_4$ solution. *Chem Eng J.* 2014;249:72–78.
8. Martinez AI, Deshpande BK. Kinetic modeling of H_2O_2-enhanced oxidation of flue gas elemental mercury. *Fuel Process Technol.* 2007;88:982–987.
9. Ye, QF. Gaseous Mercury Absorption from Simulated Flue Gas, vol. 1. Hangzhou: Zhejiang University, 2006:6–16.
10. Ma XY. Experimental Study on Removal Mercury from Flue Gas by Aqueous Solution, vol. 1. Baoding: North China Electric Power University, 2007:3–15.
11. Tan YW, Lu D, Anthony EJ, Dureau R. Mercury removal from coal combustion by Fenton reactions–Paper B: pilot-scale tests. *Fuel.* 2007;86:2798–2805.
12. Iverfeldt Å, Lindqvist O. Atmospheric oxidation of elemental mercury by ozone in the aqueous phase. *Atmos Environ.* 1986;8:1567–1573.
13. Li Y, Murphy P, Wu CY. Removal of elemental mercury from simulated coal-combustion flue gas using a SiO_2–TiO_2 nanocomposite. *Fuel Process Technol.* 2008;89:567–573.
14. Granite EJ, Pennline HW. Photochemical removal of mercury from flue gas. *Ind Eng Chem Res.* 2002;41:5470–5476.
15. Granite EJ, King WP, Stanko CD, Pennline HW. The implications of mercury interactions with band-gap semiconductor oxides. *Main Group Chem.* 2008;7:227–237.
16. Granite EJ, Pennline HW, Hoffman JS. Effects of photochemical formation of mercuric oxide. *Ind Eng Chem Res.* 1999;38:5034–5037.
17. McLarnon CR, Granite EJ. Pennline, HW. The PCO process for photochemical removal of mercury from flue gas. *Fuel ProcessTechnol.* 2005;87, 85–89.
18. Liu YX, Zhang J, Sheng CD. Simultaneous removal of NO and SO_2 from coal-fired flue gas by UV/H_2O_2 advanced oxidation process. *Chem Eng J.* 2010;162:1006–1011.
19. Neamtu M, Yediler A, Siminiceanu I. Oxidation of commercial reactive azo dye aqueous solutions by the photo-Fenton and Fenton-like processes. *J Photochem Photobiol A.* 2003;161:87–93.
20. Zhang DL, Huang YP, Luo GF, Liu DF. Research Progcess of Fenton and Photo-Fenton Reaction. *Environ Chem.* 2006;25:121–127.
21. Liu YX, Pan JF, Zhang J, Tang AK, Liu Y. Study on mass transfer-reaction kinetics of NO removal from flue gas by using UV/Fenton-like reaction. *Ind Eng Chem Res.* 2012;51:12065−12072.
22. Liu YX, Zhang J, Pan JF, Tang AK. Investigation on removal of NO from SO2-containing simulated flue gas by UV/Fenton- like reaction. *Energy Fuels.* 2012:26:5430−5436.
23. Zhang CF. Gas-Liquid Reaction and Reactor, vol. 1. Beijing: Chemical Industry Press, 1985:1−6.
24. Liu YX, Zhang J, Sheng CD. Kinetic model of NO removal from SO_2-containing simulated flue gas by wet UV/H_2O_2 advanced oxidation process. *Chem Eng J.* 2011;168:183–189.
25. Sauer MCJ, Brown WG, Hart, EJ. O(^{3}P) atom formation by the photolysis of hydrogen peroxide in alkaline aqueous solutions. *J. Phys Chem.* 1984;88:1398−1400.
26. Chang MW, Chung CC, Chern JM. Dye decomposition kinetics by UV/H_2O_2: initialrate analysis by effective kinetic modelling methodology. *Chem Eng Sci.* 2008;40:154–159.
27. Rauf MA, Marzouki N. Photolytic decolorization of Rose Bengal by UV/H_2O_2 and data optimization using response surface method. *J Hazard Mater.* 2008;159:602–609.
28. Li L, Gao NY, Hu L, Zhao JF, Li YD. The inflence of inorganic anions on bisphenol A degradation by combination of UV/H_2O_2/micro-aeration process. *China Environ Sci.* 2008;28:233–236.
29. Daneshvar N, Behnajady MA, Mohammadi MK. UV/H_2O_2 treatment of Rhodamine B in aqueous solution: influence of operational parameters and kinetic modeling. *Desalination.* 2008;230:16–26.
30. Liu YX, Wang Q. Removal of elemental mercury from flue gas by thermally activated ammonium persulfate in A bubble column reactor. *Environ Sci Technol.* 2014;48:12181−12189.
31. Liu, YX. Study on integrated desulfurization and denitrification by UV/H_2O_2 advanced oxidation process, vol. 1. Nanjing: Southeast University, 2011:10–18.
32. Zamora PL, Villamena FA. Theoretical and experimental studies of the spin trapping of inorganic radicals by 5,5-Dimethyl-1-pyrroline N-Oxide (DMPO). 3. sulfur dioxide, sulfite, and sulfate radical anions. *J Phys Chem A.* 2012;116:7210−7218.
33. Liu YX, Zhang J, Wang ZL. A study on kinetics of NO absorption from flue gas by using UV/Fenton wet scrubbing. *Chem Eng J.* 2012;197:468–474.
34. Liu YX, Pan JF, Tang AK, Wang Q. A study on mass transfer-reaction kinetics of NO absorption by using UV/H_2O_2/NaOH process. *Fuel.* 2013;108:254–260.
35. Liu YX, Zhang J. Photochemical oxidation removal of nitric oxide and sulfur dioxide from simulated flue gas of coal-fired power plants by wet scrubbing using UV/H_2O_2 advanced oxidation process. *Ind Eng Chem Res.* 2011;50:3836–3841.

Manuscript received July 15, 2014, and revision received Dec. 19, 2014.